Progress In Electromagnetics Research B, Vol. 59, 181–191, 2014

Effect of Snow Density Irregularities on Radar Backscatter from a Layered Dry Snow Pack

Boris S. Yurchak*

Abstract—The contribution of electromagnetic wave scattering on density irregularities in the volume component of radar backscatter was analyzed for a thick snow pack containing internal hoar/ice layers. To evaluate the effect of this scattering, Density Deviation Factor (DDF), a statistical parameter, was introduced into the backscattering coefficient using the "slice" approach. DDF is proportional to the intensity of the density fluctuation and inverse to the mean density. The inverse dependence of backscatter with accumulation rate was discussed based on the DDF parameterization of snow inhomogeneities.

1. INTRODUCTION

Radar techniques are often used for snow studies and monitoring in polar regions because of their ability to penetrate into a snow pack and their promise for determining snow parameters, such as the snow accumulation rate, that play an essential role in ice sheet mass-balance assessment. Another advantage of microwave radar is that it can probe the snow cover under all weather conditions, independent of season and sun illumination (i.e., day and night). However, the physical phenomenon governing the backscattering from a thick snow cover is a complicated problem, due to the complex behaviour of microwave interaction with the scattering medium. The numerous field sampling studies (e.g., [1–3]), the observations of the ground penetration radar soundings (e.g., [4, 5]) and airborne altimeters (e.g., [6]) indicate the snow pack has a layered structure. This stratification results from seasonally discontinuous accumulation of snow at the surface and from changes in meteorological conditions. Density changes observed in the dry snow zone are primarily due to the pressure exerted by the annual accumulation of snow above a layer [7] and partly due to the development of intermittent layers of depth hoar and ice lenses [3]. The interest in creating an adequate radar model of a layered, thick snow pack is the ability to remotely measure important snow balance features, such as snow accumulation rate. Existing models of the backscatter from a layered snow pack are based on the incoherent summation of individual returns or multi scatterings from grains and/or layers (e.g., [8–16]). For example: Bingham and Drinkwater [13] used a radiative transfer (RT) approach and contributed the volume backscatter from a single annual layer of a firn as the incoherent sum of independent spherical scatterers. The backscatter coefficient is strongly dependent on the grain sizes and layer thickness (accumulation). The backscattering-accumulation inverse relationship is due to increasing of the layer loss factor with increasing layer thickness (accumulation) and decrease in the net size of grains. Forster et al. [12] also exploited the RT approach with the Dense Media RT (DMRT) correction on near-field effects causing the coherent scattering between the closely located individual grains. This correction was expressed through so-called optically equivalent snow grain radius that decreases the sensitivity of the backscatter coefficient to the lager grain size. The primarily interpretation of the observable inverse backscattering-accumulation relationship was based on theoretically modeled decreasing grain size with increasing the accumulation rate. These models showed some success but fail to adequately explain many of the

Received 24 February 2014, Accepted 8 April 2014, Scheduled 11 April 2014

* Corresponding author: Boris S. Yurchak (yurboris@umbc.edu).

The author is with the Goddard Earth Sciences and Technology Center, University of Maryland, Baltimore County, Baltimore, MD 21228, USA.

observed results (e.g., [14, 17, 18]). The essential common shortcoming of models basing on incoherent summation of backscattering from snow particles consists in the following. The models produce a non-zero value of the backscatter coefficient even if all snow particles have the same size and their concentration is not varied within the whole scattering volume, i.e., when snow pack has a "frozen" (solidified) structure. In such case, the pack has no stratification and is close to homogeneous dielectric. From the physical point of view, such body cannot produce any backscatter if sizes of scattering particles and a distance between them are less than the wavelength of illuminating electromagnetic irradiance. The current paper will address this problem by taking into account the medium inhomogeneities, as the additional (alternate) contributor to radar backscatter by using the "slice" approach, which was suggested earlier in weather radar meteorology [19, 20] but has received little attention since. In the present work, the theoretical techniques that have been suggested for atmospheric clouds, and further generalized and developed for spatially extended geophysical targets in [21], will be utilized. The analysis primarily focuses on assessing the contribution of density irregularities originating from internal hoar and ice layers within a snow pack. In particular, such information is crucial for the interpretation of data obtained from altimetry, Synthetic Aperture Radar (SAR) and scatterometry observations. Based on the evaluation, an alternate interpretation of observable inverse dependence between snow accumulation rate and radar backscatter will be proposed.

2. FIELD RADAR DATA VERSUS SNOW DENSITY CHARACTERISTICS

There are several studies providing experimental data of radar soundings of snow where the impact of snow density inhomogeneities on the radar backscatter was observed. The pioneering work was carried out in [22] where an S-band (2 GHz) ground based radar with a pulse duration of approximately 1 nsec was used for sounding a snow pack of 1.7 m depth. Qualitative results regarding the origin of the backscatter were obtained in this study. It was stated that the variation in density affects the radar return; the peaks in the reflected signal corresponded to high density gradients and were not necessarily indicative of a high absolute value of density. The relationship between the electromagnetic scattering properties and physical properties of a snow pack using an FM-CW radar operating in the frequency range of 8–12 GHz with a range resolution of approximately 3 cm was studied in [23]. The data provided show an evident correlation between the density gradient and the backscatter, and weak correlation between the return amplitude and the density itself. Data from the ESA Airborne SAR/Interferometric Radar Altimeter System (ASIRAS, Ku-band, range resolution $\sim$8.8 cm in air), presented in [6] and obtained over the dry snow zone of Greenland, demonstrate obvious correspondence between the density gradient and the backscatter. Results of experimental study of backscatter sources at 800 MHz (UHF-band) and 9.3 GHz (X-band) from a region of superimposed ice and firn indicate that the reflection horizons (at UHF-band) correspond to the firn-ice interfaces where changes in permittivity occurred [5]. The actual ice body (high absolute permittivity) generates a low backscatter in both bands. The scattering at X-band tended to be stronger in the areas where a high variation of small-scale permittivity presumably exists. In a study performed in [2], measurements of density and dielectric constant were carried out in 0.5 cm increments accompanied with assessment of accumulation rate and Radarsat SAR (C-band) probing. The results demonstrate a satisfactory positive correlation ($R \approx 0.5$) between the backscatter coefficient and the standard deviation of the dielectric constant, as well as a low negative correlation (-0.1 to -0.28) with the mean dielectric constant. This study concludes that distinct inhomogeneities of the snow pack, inherent to low accumulation rate, generate a stronger backscatter. Thus, the examples above demonstrate qualitatively the significant effect of medium inhomogeneities on the formation of radar backscatter. The following evaluation is proposing a "slice" approach for the parameterization this effect in terms of the radar backscatter coefficient.

3. APPLICATION OF 'SLICE" APPROACH FOR SNOW PACK

3.1. "Slice" Approach for Snow Point Scatterers

The slice approach [19, 20] can be applied to any spatially extended geophysical target (SEGT), including snow, that contains great number of elementary scatterers and is semitransparent to the incident

electromagnetic wave. An assumption that particles located close to the front of the propagated wave are approximately at the same distance from the radar is the core of this approach. Thus, elementary radar returns arrive at the antenna nearly in the same phase (i.e., the scattering is coherent). One can imagine that these particles are embedded in a fictitious thin, cylindrical volume ("slice"), which has a base that coincides with the surface of the spherical wave front and is side-bounded by the main lobe of the antenna pattern. A slice's radial size (δ) is much narrower than the radar wavelength (λ) in the direction of wave propagation ($\delta \ll \lambda$). Representing the scattering volume of the SEGT as an adjoining series of slices, it was shown in [21] that the volume component of the backscatter is the incoherent sum of the radar cross-sections of individual scatterers only when the number of particles in the slices, n, is distributed in accordance with the Poisson law. Otherwise, the "classical" volume component should be corrected by a deviation factor $Y(\xi_a, \chi)$:

$$\langle \sigma_v \rangle = \langle \sigma_v \rangle_{class} Y(\xi_a, \chi), \tag{1}$$

where

$$Y(\xi_a, \chi) = \left(\xi_a^2 + \chi\right) / \left(\xi_a^2 + 1\right), \tag{2}$$

$\chi = Var(n)/\langle n \rangle$ is the Poisson index, $\xi_a = Stdev(a)/\langle a \rangle$ the variation coefficient of the particle radar equivalent length, $a = \sqrt{\sigma_p}$, and σ_p the radar cross-section of an individual particle. As can be concluded from (2), the decreasing backscatter can be explained by the homogeneous microstructure of dry snow, which has approximately identical particle sizes ($\xi_a \ll 1$) and negligible variations of the particle concentration ($\chi \ll 1$) within the scattering volume [24]. This supposition does not contradict with known field data, which often show low backscatter from areas with permanently dry firn and comparatively homogeneous snow morphology (e.g., [25]). It is our purpose in the present paper to extend this approach to layered snow medium.

3.2. Slice Approach for Layered Snow Medium

3.2.1. Geometrical Considerations

Following [14], the snowpack is characterized as a series of evenly-spaced rough hoar layers of random thickness. The schematic diagram for the radar sounding of a layered medium, representing the slice approach, is depicted in Figure 1. Let us assess an area, A, of a horizontal layer, L, that intersects with a slice, *sl*. To satisfy the radiophysical criterion of the infinitesimal phase shift, $\Delta\varphi \leq \pi/8$, for two-way propagation, the radial size of a slice, δ, should be equal to $\lambda/32$. The outer radius, $r_j = 0.5\Delta_j$, of a disk-like surface, S_{jj}, located at depth h_j within a slice, sl_j, can be determined from the following relationship, which follows from Figure 1:

$$(H_0 + h_j + \delta)^2 = (H_0 + h_j)^2 + r_j^2. \tag{3}$$

Because $\delta \ll H_0$, h_j and $h_j \ll H_0$, we can say that: $r_j = \sqrt{2(H_0 + h_j)\delta} \approx \sqrt{2H_0\delta}$ and $A_{jj} = \pi \cdot r_j^2 = 2\pi H_0 \delta$. In the general case, the intersection of the j-th slice with horizontal layer L_i creates an annulus, S_{ij}. The width and axial radius of the annulus can also be determined from Figure 1 based on the following relationships: $\rho_{ij} - 0.5\Delta_{ij} = \sqrt{(H_0 + h_j)^2 - (H_0 + h_i)^2}$ and $\rho_{ij} + 0.5\Delta_{ij} = \sqrt{(H_0 + h_j + \delta)^2 - (H_0 + h_i)^2}$. Because the annulus width of the intersection of layer L_i with slice sl_j depends on two depths, h_i and h_j, the corresponding width has the double index (ij). The same is true for the axial radius ρ_{ij}. Because $\delta \ll H_0$ and h_j, $h_i \ll H_0$, and assuming that the distance between the depth of the central point f_j (h_j) and depth of the layer (h_i) is much greater than the radial size of a slice, $\delta/(h_j - h_i) \ll 1$, it is possible to obtain the following expressions from the relationships provided above: $\Delta_{ij} \approx \delta\sqrt{0.5H_0/(h_j - h_i)}$ and $\rho_{ij} \approx \sqrt{2H_0(h_j - h_i)}$. Thus,

$$A_{ij} = 2\pi\rho_{ij}\Delta_{ij} \approx 2\pi\, H_0\, \delta = A. \tag{4}$$

This result agrees with the estimate of A_{jj} for disk area S_{jj} of a layer L_j, provided above. As seen by (4), the areas of intersection do not depend on a layer's depth and are approximately the same for all layers. For ordinary spatial extension of radar incidence pulses, the backscattering volume includes the entire depth of a snow pack down to rock bottom or to the penetration depth (D_p). Consequently, the backscatter arrives at the radar antenna from all slices within a pack simultaneously. The number

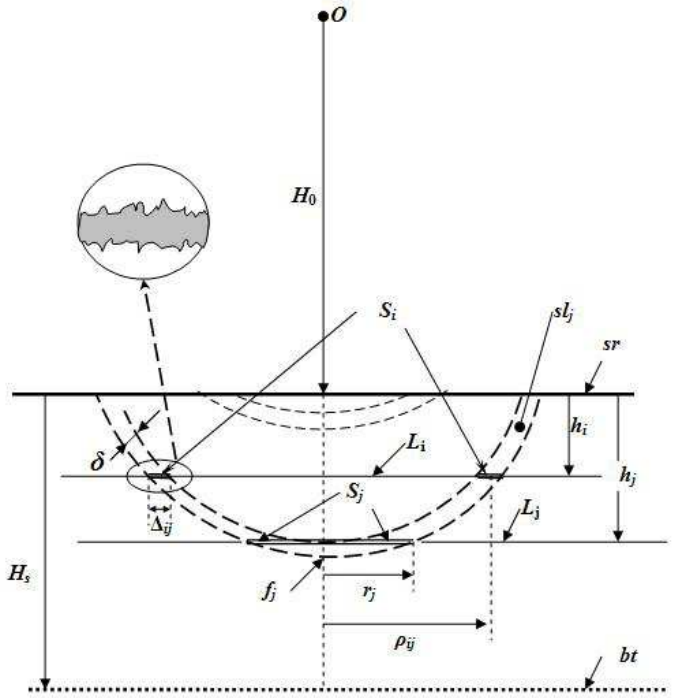

Figure 1. Schematic diagram of radar sounding of a thick layered snowpack using the slice approach. O is a radar location in an orbit of height H_0. sl_j is a cross-section of a slice with radial size δ. L_i is a layer located at depth h_i under the surface sr. S_{ij} is a cross-section of an annulus at the intersection of a layer L_i with a slice sl_j. f_j is the central point of slice sl_j. Δ_{ij}, r_j and ρ_{ij} are the width, outer radius and an axial radius, respectively, of the disk/annulus of intersection of slice sl_j with a layer L_i. L_j is the deepest layer of a slice sl_j. h_j is the depth of layer L_j and of central point f_j. S_{jj} is a cross-section of a disk area at the intersection of the deepest layer L_j with the slice sl_j. H_s is the depth of a snow pack, and bt is the bottom of the snow pack.

of layers intersecting an individual slice depends on the location of the central point of a slice (point f). This number might be greater if the central point location is deeper inside a snow pack, the layers are uniformly distributed along the depth and are continuously extended in a horizontal plane within the illumination spot of the main lobe of the antenna pattern. On the other hand, the deeper intersection areas generate lower magnitude return signals due to attenuation. Due to these reasons and some other factors determining the "filling" of slices, the contribution of all slices will be considered, in the first approximation, as equal and independent of the depth of their central points. To qualitatively take into account the unevenness of the contribution of particular slices in the total backscatter, the number of effective slices, N_s, is introduced, instead of theoretically estimating the total number of slices ($\sim D_p/\delta$). A slice intersected with one layer, at least, is conditionally considering as an "effective".

3.2.2. Radar Backscatter Coefficient versus Statistics of Density Irregularities

As shown earlier in [21], the total mean radar cross section of the scattering volume for point scatterers is

$$\langle \sigma_\Sigma \rangle = Var(b) M_{eff}, \tag{5}$$

where b is the slice radar equivalent length (SREL) which is equal to the sum of all field backscatters from individual particles ($\sqrt{\sigma_p}$) within a slice. M_{eff} is the effective number of slices within the scattering

volume. When analyzing a layered medium, the SREL of j-th slice can be expressed in the form:

$$b_j = \sum_{i=1}^{N_j} \sqrt{\sigma_{ij}}, \tag{6}$$

where σ_{ij} is the radar cross section of the intersection area A_{ij} of the i-th layer with a j-th slice, and N_j is the number of layers intersecting with the j-th slice. Dividing the left and right parts of Equation (6) by the square root from intersection area (A), defined by Equation (4), which is the same for all layers, a slice field backscattering coefficient (SFBC) can be written:

$$b_j^0 \equiv b_j \Big/ \sqrt{A} = \sum_{i=1}^{N_j} \sqrt{\sigma_{ij}^0}, \tag{7}$$

where $\sigma_{ij}^0 \equiv \sigma_{ij}/A$ is a backscattering coefficient of an intersection area A_{ij}. Following [8, 26], the backscattering coefficient from A_{ij} for normal incidence can be written in the general form:

$$\sigma_{ij}^0 = \alpha_{ij}^2 \Gamma_{ij}^2, \tag{8}$$

where α_{ij}^2 is a coefficient depending on the roughness of area A_{ij}, and on small deviation of incidence angle from vertical (within a half of the angular width of main lobe of antenna pattern) for peripheral parts of a layer. Γ_{ij} is the Fresnel reflection coefficient of this area under vertical incidence. Equation (8) assumes the horizontal electrical homogeneity within the scattering volume (the Fresnel coefficient is the same for the whole annulus). Certainly, the Fresnel coefficient and factor α can also vary for different layers and slices. Since the slice approach presupposes coherent scattering from all reflection elements within a slice, it is assumed that phase shifts upon scattering from intersection areas are not greater than radiophysical criterion of the infinitesimal phase shift, $\Delta\varphi \leq \pi/8$. In accordance with [27], the buried annual layer boundaries often meet this criterion under roughness conditions for C-band $k \cdot Stdev(h) \leq 0.3$ ($k = 2\pi/\lambda$ is the wavenumber for wavelength λ and h is the surface height). At that, the backscatter coefficient is dominated by the specular component at angles near normal incidence [28]. Substituting expression (8) in Equation (7), the SFBC for the j-th slice can be written through the parameters of intersection areas:

$$b_j^0 = \sum_{i=1}^{N_j} \alpha_{ij} \, |\Gamma_{ij}|. \tag{9}$$

Following the method of calculation evaluated earlier in [21] under the slice approach for point scatterers, the mean backscattering coefficient for the layered medium may be expressed in the form similar to Equation (5):

$$\left\langle \sigma_L^0 \right\rangle = Var(\alpha\Gamma) N_s. \tag{10}$$

If geometric features of irregularities do not correlate with the electrical properties of a layer surface, the mean value of the scattering coefficient can be expressed through the following combination of statistics of parameter α and the Fresnel coefficient Γ:

$$\left\langle \sigma_L^0 \right\rangle \approx \Big\{ Var\,(\alpha)\; Var(\,\Gamma) + \langle\alpha\rangle^2\; Var(\,\Gamma) + \langle\Gamma\rangle^2\; Var\,(\alpha) \Big\}\; N_s. \tag{11}$$

It is difficult to take into account variations of α and the Fresnel coefficient at the same time. Thus, only the simplest case, similar irregularities for all layers within the scattering volume (i.e., $\alpha = \text{const}$), is under the current consideration. This assumption leads to the following expression for the layered component of the backscattering coefficient:

$$\left\langle \sigma_L^0 \right\rangle \approx \alpha^2 \, Var(\Gamma) N_s. \tag{12}$$

Equation (12) means that the source of the layer component of the backscatter is the variation of the Fresnel coefficient within the snow pack. Therefore, to evaluate, in the first approximation, the backscatter from a layered snow structure, it is necessary to analyze the variance of the electrical properties of layers expressed through the Fresnel coefficient.

4. VARIATION OF THE FRESNEL COEFFICIENT FOR DENSITY LAYERS

4.1. Reflection Model of Snow/Firn Density Layer

The polar firn consists of numerous layers of different density, which have thickness on the order of centimeters (e.g., 1 to 3 cm determined in [29], 3 to 6 cm determined in [10]) and gaps between the layers from tens of centimeters to meters, e.g., [2, 3]. Boundaries between a layer and background snow include transition zones, Figure 2. Therefore, we can consider the snow pack as a series of borders and layers with a variety of snow and firn densities.

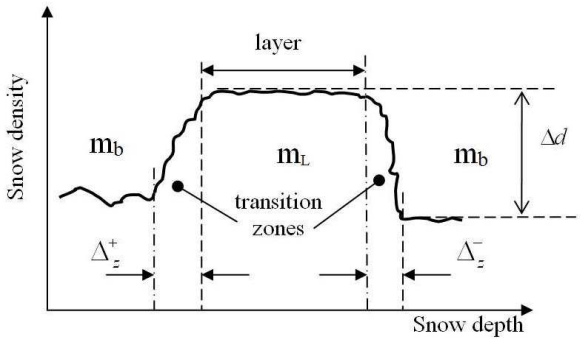

Figure 2. A schematic diagram of a snow layer with increased density. $\Delta_z^{+/-}$ is the radial size of the transition area contacted with upper (+) and lower (−) parts of a layer, respectively; $m_{L,b}$ is the refractive index of a layer and background snow, respectively; Δd is the density difference between a layer and background snow.

4.2. Modification of the Fresnel Coefficient due to the Finite Size of the Transition Zone

Let us consider the Fresnel reflection coefficient for incidence angles of zero and smooth surface. For a discontinuous ("sharp") change of the reflection coefficient that occurs in a distance $\Delta_z < \lambda/4$, the square of the reflection coefficient is (e.g., [30]):

$$\Gamma_0^2 = \left| \frac{\dot{m}_L - \dot{m}_b}{\dot{m}_L + \dot{m}_b} \right|^2, \tag{13}$$

where $\dot{m}_{L,b}$ is the complex refractive index of a layer and background snow. Assuming dry snow and small changes in the absolute values of m between a layer and surrounded snow, we have only the real values of the indices and $m_L \approx m_b \approx m$. Hence, one can write:

$$\Gamma_0^2 \approx (0.5\Delta m/m)^2, \tag{14}$$

where Δm is the step-like variation of the refractive index across the border between two mediums. However, variations in the refractive index of a real snow medium can hardly be assumed to be sharp, i.e., to occur within a distance that is much less than the wavelength. These changes are effective within some length (transition zone, Figure 2) and can be either linear or not linear. The corresponding variations of the reflection coefficient can be taken into account by the correction coefficient g. This coefficient depends upon the ratio of the transition zone thickness (Δ_z) to the wavelength (λ) and on the profile of refractive index within the interval Δ_z [31]. Thus, in general case, the Fresnel coefficient for a layer may be written in the form:

$$\Gamma^2 = g^2 \cdot \Gamma_0^2. \tag{15}$$

To simplify further consideration, the correction coefficient (g) will be assumed to be a constant for all layers within a snow pack.

4.3. Variance of the Fresnel Coefficient versus Statistics of Snow Dielectric Permittivity

As follows from (12), the backscatter depends on the fluctuation of the reflection coefficient, Γ, or fluctuations in the gradient of the refractive index. Following [30], the Fresnel reflection coefficient

for dry snow can be written in the form: $\Gamma_0^2 = (0.25\Delta\varepsilon/\varepsilon)^2$, where ε is a dielectric permittivity (this follows from (14) due to $m = \sqrt{\varepsilon}$). Consequently, taking into account Equation (14), the variance of the reflection coefficient (15) can be expressed through the variance of relative fluctuations of a snow permittivity

$$Var\left(\Gamma\right) = g^2 \frac{1}{4} Var\left(\frac{\Delta m}{m}\right) = \left(\frac{g}{4}\right)^2 Var\left(\frac{\Delta\varepsilon}{\varepsilon}\right). \tag{16}$$

In accordance with the rules of statistics (e.g., [32]), the variance of the relative dielectric permittivity in (16) for independent deviation ($\Delta\varepsilon$) and absolute values (ε) can be transformed as follows:

$$Var\left(\frac{\Delta\varepsilon}{\varepsilon}\right) \approx \frac{1}{\langle\varepsilon\rangle^2} Var\left(\Delta\varepsilon\right) + \langle\Delta\varepsilon\rangle^2 \frac{1}{\langle\varepsilon\rangle^4} Var\left(\varepsilon\right). \tag{17}$$

To compare the contribution of each term in expression (17), the variation of the permittivity deviation in the first term can be represented as $Var(\Delta\varepsilon) = Var\left(\langle\varepsilon\rangle - \varepsilon\right) = Var(\langle\varepsilon\rangle) + Var(\varepsilon)$. For a number of irregularities $p \gg 1$, $Var(\langle\varepsilon\rangle) = p^{-1} Var(\varepsilon) \ll Var(\varepsilon)$ and expression (17) can be written in the form:

$$Var\left(\frac{\Delta\varepsilon}{\varepsilon}\right) \approx \frac{Var\left(\varepsilon\right)}{\langle\varepsilon\rangle^2}\left(1 + \frac{\langle\Delta\varepsilon\rangle^2}{\langle\varepsilon\rangle^2}\right). \tag{18}$$

Known observations of layered snow stratigraphy (e.g., [3]) show most transitions of dielectric permittivity pertained to layers which exceed the permittivity of surrounding media due to higher density. Because of that $\langle\Delta\varepsilon\rangle > 0$. However, these data indicate that $\langle\Delta\varepsilon\rangle^2 \ll \langle\varepsilon\rangle^2$, and thus the term in the brackets equals approximately to 1. Finally,

$$Var\left(\Gamma\right) \approx \left(\frac{g}{4}\right)^2 \frac{Var\left(\varepsilon\right)}{\langle\varepsilon\rangle^2}. \tag{19}$$

4.4. Variance of the Fresnel Coefficient versus Variance of Snow Density

Based on the analysis of dry snow under significant negative temperatures, only the real part of the dielectric permittivity will be taken into account. The dependence of the dielectric permittivity on values of snow density (d) less than $0.5\,\mathrm{g/cm^3}$ can be represented by a linear function in accordance with [33]:

$$\varepsilon = 1 + q \cdot d, \tag{20}$$

where d is the snow density in $\mathrm{g/cm^3}$ and q is a fitting coefficient equal to $(1.9\text{–}2.2)\,\mathrm{cm^3/g}$. Since $Var(\varepsilon) = Var(qd)$, we can write:

$$\frac{Var\left(\varepsilon\right)}{\langle\varepsilon\rangle^2} = \frac{Var\left(qd\right)}{\langle 1 + qd\rangle^2} = \frac{Var\left(qd\right)}{\left(1 + \langle qd\rangle\right)^2} \equiv \xi_d^2, \tag{21}$$

and Equation (19) can be expressed by snow density statistics:

$$Var\left(\Gamma\right) = \left(\frac{g}{4}\right)^2 \xi_d^2, \tag{22}$$

where ξ_d^2 is the Density Deviation Factor (DDF). If $\langle qd\rangle \ll 1$, then $\xi_d^2 \approx Var(qd)$. Combining relationships (12) and (22), the following expression for the volume layer subcomponent of the backscatter coefficient for nadir sounding yields:

$$\left\langle\sigma_L^0\right\rangle = \left(\alpha\frac{g}{4}\right)^2 N_s \xi_d^2. \tag{23}$$

Thus, the backscatter coefficient of a layered snow medium is proportional to the intensity of the density fluctuation through the DDF (ξ_d^2). This is an analytical expression of known experimental fact that a pronounced stratification, causing by depth hoar/ice layers and other density irregularities, resulted in greater backscatter (e.g., [25]). From the backscattering coefficient Equation (23), the absolute value of a layered component is determined, in addition to the DDF, by a factor, $(\alpha g/4)^2 N_s$, that might be further assessed by a calibration or theoretical consideration that is currently outside the scope of this analysis.

4.5. Remarks regarding Non-Vertical Incidence

The analysis above was conducted for incidence angles of radar irradiation that are close to vertical (nadir). This pattern is peculiar primarily to altimetry. For scatterometry and SAR, the direction of sounding differs from the nadir. That changes the definitions of some parameters in Equation (23). An angle of incidence must be taken into account upon assessment of the coefficients Γ, α and g. It should be mentioned that the backscatter contains also a depolarization component. The number of effective slices, N_s, and DDF (density stratification) should be determined along a slant range in the probing direction. More detailed development of the approach for this case might be fulfilled later.

5. SNOW DENSITY IRREGULARITIES VERSUS MEAN DENSITY AND ACCUMULATION RATE

5.1. Density Variations versus Mean Density

As was shown above in Equation (21), the variation and mean of density govern the DDF. As shown in numerous field studies, the density variation decreases as the mean density increases (e.g., [34]). The behaviour of DDF, calculated in accordance with Equation (21), with $q = 2.0\,\mathrm{cm}^3/\mathrm{g}$, and based on field data available in the literature, is depicted in Figure 3. This plot demonstrates the obvious decrease in DDF versus the mean density due to the densification process. Thus, the primary contribution to the layered backscatter is caused by the upper part of a snow pack. Because of that, the field data acquired with ordinary subsurface density measurements can be used for assessing the DDF.

5.2. Density Irregularities versus Accumulation Rate

A detailed field study of density variations as a function of the accumulation rate was conducted in [39]. The density was measured continuously at 10 cm intervals in a number of firn cores collected from East Antarctica. It was found, using these data in conjunction with data collected from Byrd Station, West Antarctica [33], that the density variability on the scale of ∼1 m systematically increases, with a magnitude greater than 100–200 $\mathrm{kg{\cdot}m^{-3}}$ in the first 2 m of depth, with decreasing accumulation rate (248–70 $\mathrm{kg{\cdot}m^{-2}{\cdot}a^{-1}}$). In accordance with [40], "... the major cause of the large variability in density in the low-temperature, low-accumulation region is the time of exposure to temperature gradients." This period is longer for low-accumulation sites. Each deposited firn layer remains near the surface and exposed to the extreme temperature gradient for a longer period producing greater irregularities. The plot of the calculated DDF, as a function of the accumulation rate, based on the data about the density variance on the scale of 2–4 cm, for sites in Greenland and the Antarctic (after [37]) is shown in Figure 4. In accordance with the plot, an area with high snow accumulation produces a lower DDF compared to an area with a low snow accumulation rate. The corresponding DDF gradient is $\frac{\mathrm{DDF_{dB}}}{\Delta \mathrm{Acc}} = (3.2 \pm 0.5) \cdot 10^{-2}$,

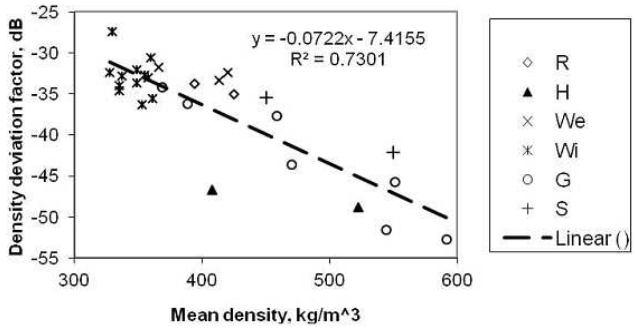

Figure 3. Statistical relationship between density deviation factor and mean snow density calculated using data from several authors. (Legend: R — [35], H — [36], We — [29], Wi — [37], G — [34], S — [38]).

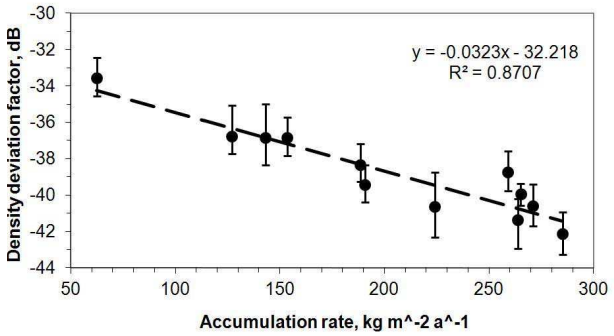

Figure 4. Density deviation factor versus snow accumulation rate calculated based on the 2–4-cm-scale variation of firn density data (after [37]) for sites in Greenland and the Antarctic.

$[\frac{\text{dB}}{\text{kg}\cdot\text{m}^{-2}\cdot\text{a}^{-1}}]$. The observed relationship between radar backscatter and accumulation rates in the Greenland ice sheet based on the C-band ($\lambda_0 = 5.66\,\text{cm}$) ERS-1 SAR mosaic data [41] and the accumulation rate map (e.g., [42]) has been reported in [12]. It was shown that, within the dry snow zone of Greenland, the accumulation rates vary from approximately 40 cm year^{-1} water equivalent ($400\,\text{kg}\cdot\text{m}^{-2}\cdot\text{a}^{-1}$) in the south-west to 10 cm year^{-1} water equivalent ($100\,\text{kg}\cdot\text{m}^{-2}\cdot\text{a}^{-1}$) in the north-east. These rates were accompanied by the backscatter coefficient trend ranging from -14 to $-5\,\text{dB}$. Hence, $\frac{\Delta\sigma^0}{\Delta\text{Acc}} \sim 3.0\cdot 10^{-2}$, $[\frac{\text{dB}}{\text{kg}\cdot\text{m}^{-2}\cdot\text{a}^{-1}}]$. This gradient is in satisfactory agreement with the DDF gradient estimated above. The DDF was also assessed by results of measurements of snow density profiles in Antarctica with a spatial resolution of 5 cm and 10 cm published in [29, 35, 38]. These data demonstrate similar decreasing tendency of DDF as a function of accumulation rate. Moreover, these data, in conjunction with the backscatter measurements of the C-band scatterometer carried out in [25], also show the decrease of backscatter, by $\sim$3 dB, with an increasing accumulation rate of 90–220 $\text{kg}\cdot\text{m}^{-2}\cdot\text{a}^{-1}$. These figures produce the backscattering gradient which is within the range of DDF gradients assessed above. In a study [2], the correlation of backscatter with the accumulation rate was notably negative, approximately -0.55. The estimate of the backscatter gradient is $\sim(6.6\pm 4.3)\cdot 10^{-2}[\frac{\text{dB}}{\text{kg}\cdot\text{m}^{-2}\cdot\text{a}^{-1}}]$, which includes the gradient value for the Greenland data cited above. In conclusion, it can be stated that DDF correlates with accumulation rate inversely and DDF, therefore, partially governs the backscatter coefficient by taking into account the contribution of snow density irregularities.

6. SUMMARY

Known approaches to model radar backscatter from thick snow pack exploits incoherent summation of the radar cross section of individual scatterers (grains and/or layers) or take into account multiple-scattering effects. Although the inhomogeneities of snow structure are commonly accepted as a possible source of the backscatter, none of the existing models include parameters that characterize the contribution of these inhomogeneities to the radar backscatter. In the present consideration, an approach to assess the volume component of the radar backscatter, based on parameterization of snow density irregularities, is suggested. Applying the slice approach, which was previously used to describe the backscatter from extended targets containing point scatterers, the backscatter coefficient for a layered dry snow is expressed through the statistical parameter, Density Deviation Factor (DDF). This parameter takes into account the contribution from fluctuations in snow density, along the path of electromagnetic wave propagation within a snow pack, to the total scattering. An assessment of relative changes to the backscatter coefficient based on the derived statistics, does not contradict the backscatter behavior of observable field data available in the literature. In accordance with the suggested model, the inverse trend of the return signal strength to the accumulation rate can be caused by relatively low values of snow density variations within the scattering volume and, consequently, low DDF, which are inherent in areas with high accumulation rates. Some factors impacted the radar backscatter, which were ignored in the current consideration for simplification purposes, are not critical to the main result and might be taken into account by the further improvement of this statistical approach.

ACKNOWLEDGMENT

This work was supported by the NASA Cryospheric Science Program. The author is grateful to an anonymous reviewer for useful comments, which improved the manuscript.

REFERENCES

1. Shuman, C. A., D. H. Bromwich, J. Kipfstuhl, and M. Schwanger, "Multiyear accumulation and temperature history near the North Greenland Ice Core Project site, north central Greenland," *J. Geophys. Res.*, Vol. 106, No. D24, 33853–33866, 2001.
2. Zahnen, N., F. Jung-Rothenhausler, H. Oerter, F. Wilhelms, and H. Miller, "Correlation between Antarctic dry snow properties and backscattering characteristics in radarsat SAR imagery,"

Proceedings of EARSeL-LISSIG Workshop Observing Our Cryosphere from Space, 140–148, Bern, Mar. 11–13, 2002.

3. Kärkäs, E., T. Martma, and E. Sounninen, "Physical properties and stratigraphy of surface snow in western Droning Maud Land, Antarctica," *Polar Research*, Vol. 24, Nos. 1–2, 55–67, 2005.
4. Godio, A., "Georadar measurements for the snow cover density," *American Journal of Applied Sciences*, Vol. 6, No. 3, 414–423, 2009.
5. Langley, K., P. Lacroix, S.-E. Hamran, and O. Brandt, "Sources of backscatter at 5.3 GHz from a superimposed ice and firn area revealed by multi-frequency GPR and cores," *J. Glaciology*, Vol. 55, No. 190, 373–383, 2009.
6. Hawley, R. L., E. M. Morris, R. Cullen, U. Nixdorf, A. P. Shepherd, and D. J. Wingham, "ASIRAS airborne radar resolves internal annual layers in the dry-snow zone of Greenland," *Geoph. Res. Lett.*, Vol. 33, L04502, 2006, Doi: 10.1029/2005GL025147.
7. Kanagaratnam, P., S. P. Gogineni, N. Gundestrup, and L. Larsen, "High resolution radar mapping on internal layers at the North Greenland Ice Core Project," *J. Geophys. Res.*, Vol. 106, No. D24, 33799–33811, 2001.
8. Ulaby, F. T., R. K. Moore, and A. K. Fung, *Microwave Remote Sensing, Active and Passive, from Theory to Applications, Volume III,* Artech House, Inc., Norwood, 1986.
9. Fung, A., *Microwave Scattering and Emission Models and Their Applications*, Artech House, New York, 1994.
10. Wismann, V., D. P. Winebrenner, K. Boehnke, and R. J. Arthern, "Snow accumulation on Greenland estimated from ERS scatterometer data," *Proceedings of the IGARSS' 97*, Vol. 4, 1823–1825, Singapore, Aug. 3–8, 1997.
11. Mätzler, C., "Improved born approximation for scattering in a granular medium," *J. Appl. Phys.*, Vol. 83, 6111–6117, 1998.
12. Forster, R. R., K. C. Jezek, J. Bolzan, F. Baumgarner, and S. P. Gogineni, "Relationships between radar backscatter and accumulation rates in the Greenland ice sheet," *Int. J. Remote Sens.*, Vol. 20, Nos. 15–16, 3131–3147, 1999.
13. Bingham, A. W. and M. R. Drinkwater, "Recent changes in the microwave scattering properties of the Antarctic ice sheet," *IEEE Trans. Geosci. Remote Sens.*, Vol. 38, No. 4, 1810–1820, 2000.
14. Hoen, E. W., "A correlation-based approach to modeling interferometric radar observations of the Greenland ice sheet," Ph.D. Thesis, Stanford University, 2001.
15. Tsang, L., J. Pan, D. Liang, Z. X. Li, D. Cline, and Y. H. Tan, "Modeling active microwave remote sensing of snow using dense media radiative transfer (DMRT) theory with multiple scattering effects," *IEEE Trans. Geosci. Remote Sens.*, Vol. 45, No. 4, 990–1004, 2007.
16. Xu, X., D. Liang, L. Tsang, K. M. Andreadis, E. G. Josberger, D. P. Lettenmaier, D. W. Cline, and S. H. Yueh, "Active remote sensing of snow using NMM3D/DMRT and comparison with CLPX-II airborne data," *IEEE J. Selected Topics in Applied Earth Observations and Remote Sensing*, Vol. 3, No. 4, 689–697, 2010.
17. Kendra, J. R., K. Sarabandi, and F. T. Ulaby, "Radar measurement of snow: Experiment and analysis," *IEEE Trans. Geosci. Remote Sens.*, Vol. 36, No. 3, 864–879, 1998.
18. Ruiz, C., "Feasibility study of imaging the Antarctic ice using a space-borne P-band radar," WP 200: Electromagnetic Model Review Document, ESA Contract No. 18195/04/NL/CB, 2005.
19. Marshall, J. S. and W. Hitchfeld, "Interpretation of the fluctuating echo from randomly distributed scatterers," *Can. J. Phys.*, Vol. 31, No. 6, 962–994, 1953.
20. Smith, Jr., P. L., "Scattering of microwave by cloud droplets," *Proceedings of 11th Weather Radar Conf.*, 201–207, Boulder, Colorado, Sep. 14–18, 1964.
21. Yurchak, B. S., "Radar volume backscatter from spatially extended geophysical targets in a 'slice' approach," *IEEE Trans. Geosci. Remote Sens.*, Vol. 47, No. 11, 3690–3696, 2009, Doi: 10.1109/TGRS.2009.2015444.
22. Vickers, R. S. and G. C. Rose, "High resolution measurements of snowpack stratigraphy using a short pulse radar," *Proceedings of the 8th International Symposium on Remote Sensing of*

Environment, Vol. I, 261–267, University of Michigan, Ann Arbor, Oct. 2–6, 1972.

23. Ellerbruch, D. A. and H. S. Boyne, "Snow stratigraphy and water equivalence measured with an active microwave system," *J. Glaciology*, Vol. 26, No. 94, 225–233, 1980.
24. Yurchak, B. S., "Some features of the volume component of radar backscatter from thick and dry snow cover," *Advances in Geoscience and Remote Sensing*, G. Jedlovec (ed.), 93–140, In-Tech, Vukovar, 2009.
25. Rott, H., K. Sturm, and H. Miller, "Active and passive microwave signatures of Antarctic firn by means of field measurements and satellite data," *Ann. Glaciol.*, Vol. 17, 337–343, 1993.
26. Ulaby, F. T., R. K. Moore, and A. K. Fung, *Microwave Remote Sensing: Active and Passive, Radar Remote Sensing and Surface Scattering and Emission Theory, Volume II*, Artech House, Norwood, MA, 1992.
27. Long, D. G. and M. R. Drinkwater, "Greenland ice-sheet surface properties observed by the Seasat — A scatterometer at enhanced resolution," *J. Glaciology*, Vol. 40, 213–230, 1994.
28. Eom, H. J. and W.-M. Boerner, "A re-examination of radar terrain backscattering at nadir," *IEEE Trans. Geosci. Remote Sens.*, Vol. 24, No. 2, 232–234, 1986.
29. West, R. D., D. P. Winebrenner, L. Tsang, and H. Rott, "Microwave emission from density-stratified Antarctic firn at 6 cm wavelength," *J. Glaciology*, Vol. 42, No. 140, 63–76, 1986.
30. Paren, J. G., "Reflection coefficient at a dielectric interface," *J. Glaciology*, Vol. 27, No. 95, 203–204, 1981.
31. Atlas, D., "Advances in radar meteorology," *Adv. Geophys.*, Vol. 10, 317–478, 1964.
32. Kendall, M. G., *Advanced Theory of Statistics, Volume 1*, 6th Edition, Arnold, Stuart & Ord., London, 1968.
33. Tiuri, M. E., A. H. Sihvola, E. G. Nyfors, and M. T. Hallikainen, "The complex dielectric constant of snow at microwave frequencies," *IEEE J. Ocean. Engin.*, Vol. 9, No. 5, 377–382, 1984.
34. Gow, A. J., "Deep core studies of the accumulation and densification of snow at Byrd Station and Little America V, Antarctica," CRREL Research Report, 197, 1968.
35. Rotschky, G., W. Rack, W. Dierking, and H. Oerter, "Retrieving snowpack properties and accumulation estimates from a combination of SAR and scatterometer measurements," *IEEE Trans. Geosci. Remote Sens.*, Vol. 44, No. 4, 943–956, 2006.
36. Holmlund, P., K. Gjerde, N. Gundestrup, M. Hansson, E. Isaksson, L. Karlöf, M. Nyman, R. Pettersson, F. Pinglot, C. H. Reijmer, M. Stenberg, M. Thomassen, R. S. W. van de Wal, C. Veen, F. Wilhelms, and J. G. Winther, "Spatial gradients in snow layering and 10 m temperatures at two EPICA-Dronning Maud Land (Antarctica) pre-site-survey drill sites," *Ann. Glaciol.*, Vol. 30, 13–19, 2000.
37. Winebrenner, D. P., R. J. Arthern, and C. A. Shuman, "Mapping Greenland accumulation rates using observations of thermal emission at 4.5-cm wavelength," *J. Geophys. Res.*, Vol. 106, No. D24, 33919–33934, 2001.
38. Schlosser, E. and H. Oerter, "Shallow firn cores from Neumayer, Ekstromisen, Antarctica: A comparison of accumulation rates and stable-isotope rations," *Ann. Glaciol.*, Vol. 35, 91–96, 2002.
39. Quin, D. and N. W. Young, "Characteristics of the initial densification of snow/firn in Wilks land, east Antarctica," *Ann. Glaciol.*, Vol. 11, 209, 1988.
40. Li, J. and J. Zwally, "Modeling the density variation in the shallow firn layer," *Ann. Glaciol.*, Vol. 38, 309–313, 2004.
41. Fahnestock, M., R. Bindschadler, R. Kwok, and K. Jezek, "Greenland ice sheet surface properties and ice dynamics from ERS-1 SAR imagery," *Science*, Vol. 262, No. 5139, 1530–1534, 1993.
42. Bromwich, D. H., R. I. Cullather, and Q. Chen, "Evaluation of recent precipitation studies for the Greenland ice sheet," *J. Geophys. Res.*, Vol. 108, No. D20, 26007–26024, 1998.